PHILOSOPHICAL MAGAZINE A, 2000, VOL. 80, NO. 5, 1151–1163

Plastic deformation of icosahedral Al–Pd–Mn single quasicrystals I. Experimental results

B. GEYER†, M. BARTSCH†, M. FEUERBACHER‡, K. URBAN‡ and U. MESSERSCHMIDT*‡

† Max-Planck-Institut für Mikrostrukturphysik, Weinberg 2, D-06120 Halle/Saale, Germany
‡ Institut für Festkörperforschung, Forschungszentrum Jülich GmbH, D-52425 Jülich, Germany

[*Received 15 March 1999 and accepted in revised form 7 July 1999*]

ABSTRACT

In order to compare plastic deformation along different loading axes, icosahedral Al–Pd–Mn single quasicrystals were deformed in uniaxial compression along twofold and fivefold axes, between the lowest temperatures where deformation at strain rates of 10^{-5} and 10^{-4} s^{-1} was possible and 820°C. For the first time, experiments were performed below 680°C. The strain rate and temperature sensitivity of the flow stress were studied by stress relaxation and temperature change tests. In a range of strain of steady state deformation following a yield drop, the flow stress and its strain rate sensitivity increase strongly with decreasing temperature. The temperature sensitivity shows a maximum at about 700°C. The data hardly depend on the specimen orientation. Repeated relaxation tests indicate changes in the microstructure during the relaxations. Transient phenomena also occurred when the relaxation tests had not been started from steady state deformation, e.g. before the upper yield point, after long relaxations or after unloading. The results will be discussed in Part II of this paper.

§1. INTRODUCTION

The plastic properties of quasicrystalline materials were first investigated on polycrystals, e.g., by Shibuya *et al.* (1990), Bresson and Gratias (1993), Takeuchi and Hashimoto (1993), and Shield *et al.* (1994). The discovery of thermodynamically stable ternary quasicrystalline phases by Tsai *et al.* (1989) and the resulting possibility of growing large single quasicrystals by Yokoyama *et al.* (1992) formed the basis for the study of the intrinsic plastic properties of quasicrystals. It was shown by Wollgarten *et al.* (1993) that the dislocation density rises dramatically during the high-temperature deformation of Al–Pd–Mn single quasicrystals, pointing to a dislocation mechanism of plastic deformation. This view was confirmed by Wollgarten *et al.* (1995) by the direct evidence of dislocation motion during *in situ* deformation in a high-voltage electron microscope. The intrinsic properties of the plastic deformation of Al–Pd–Mn single quasicrystals were investigated first by

*Author for correspondence. e-mail: um@mpi-halle.mpg.de

Philosophical Magazine A ISSN 0141–8610 print/ISSN 1460-6992 online
http://www.tandf.co.uk/journals

Feuerbacher *et al.* (1995) and later by Brunner *et al.* (1997). Although these first studies give information on the activation parameters of the plastic deformation of single quasicrystals, a number of problems remain open. Different origins of the specimens and different compression axes and strain rates lead to slightly different data, the reasons for which are not yet clear. In any case, most measurements, e.g., stress relaxation tests and temperature changes, were performed at the upper yield point, owing to the (almost) constant stress a structural equilibrium was supposed. However, it was shown by Feuerbacher *et al.* (1997) that the dislocation density is increasing strongly at the upper yield point, reaching its maximum value only at the lower yield point, which means that the condition of a constant structure is violated at the upper yield point. At an intermediate deformation temperature, the dislocation density decreases during annealing to half of the initial value within about 10 min (Schall *et al.* 1999), indicating that recovery may play an important role during the deformation of quasicrystals at high temperatures. The present paper re-examines the plastic properties of Al–Pd–Mn single quasicrystals following three aims: (1) perform measurements in the plateau region after the yield drop to better fulfil the condition of constant structure; (2) enable a comparison between the deformation along twofold and fivefold compression axes; and (3) find the range of dynamic recovery at high temperatures and consider it in the interpretation. This paper describes the experimental results, which are then discussed in Part II (Messerschmidt *et al.* 2000).

§ 2. Experimental

Icosahedral single quasicrystals of the composition $Al_{70.5}Pd_{21}Mn_{8.5}$ were grown by the Czochralski technique. Rectangular specimens for compression experiments of final lengths of 5.7 or 7.8 mm and cross-sections between 2.0 mm^2 and 3.2 mm^2 were cut by spark erosion. The grip and side faces were carefully ground and polished to be plane and parallel. Samples with twofold and fivefold compression axes were cut from the same single quasicrystal. The samples with a twofold compression axis had side faces normal to pseudo-twofold and fivefold axes, those with a fivefold compression axis had side faces normal to twofold and pseudo-twofold axes. The samples were deformed in a digitally controlled single-screw testing machine in air. A linear variable differential transducer was coupled with the hot compression anvils to measure the strain. The machine was operated in closed-loop strain control, which results in a large effective stiffness. Experiments were performed at nominal or total strain rates of $\dot{\varepsilon}_t = 10^{-4}\,s^{-1}$ and $10^{-5}\,s^{-1}$ from 820°C down to the lowest temperatures where, depending on the specimen orientation and strain rate, macroscopic plastic deformation was achieved. The deformation usually is not very homogeneous. After deformation, the samples are covered with a thin, dense oxide layer, and they stick to the silicon nitride pads. Frequently, they break near the grip faces during unloading or cooling.

Figure 1 (*a*) shows a typical stress strain curve including several tests conducted during the deformation. The stress σ and the total strain ε_t are nominal stress and strain values. Stress relaxation tests (R) were performed to determine the strain rate sensitivity of the flow stress. The relaxation curves were plotted as $\ln(-\dot{\sigma})$ versus σ. In this plot, the experimental strain rate sensitivity r_{ex} is given by the inverse slope

$$r_{ex} = \Delta\sigma/\Delta \ln \dot{\varepsilon} = \Delta\sigma/\Delta \ln(-\dot{\sigma}), \qquad (1)$$

where $\dot{\varepsilon}$ is the plastic strain rate. Most data described below refer to the initial slope of the relaxation curves, i.e., they correspond to the strain rate at the beginning of the relaxation. For a special test, strain rate sensitivity values were determined also all along the relaxation curves, which correspond to decreasing strain rates. These values were obtained by piecewise fitting polynomials of second order to the relaxation curves and calculating the slopes at the centres of the pieces. Relaxation curves were measured before the upper yield point (UYP) (R1 in figure 1 (*a*)) and at or behind the lower the yield point (LYP) in a range of almost constant stress. In order

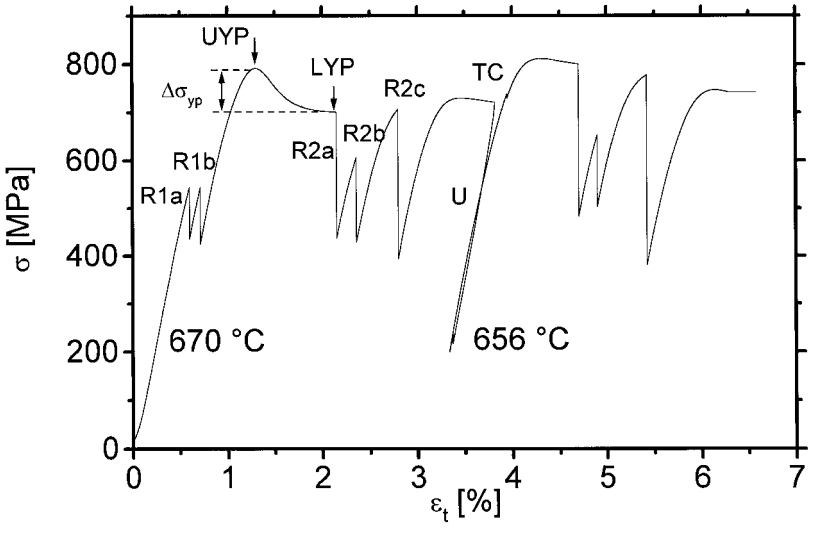

(*a*)

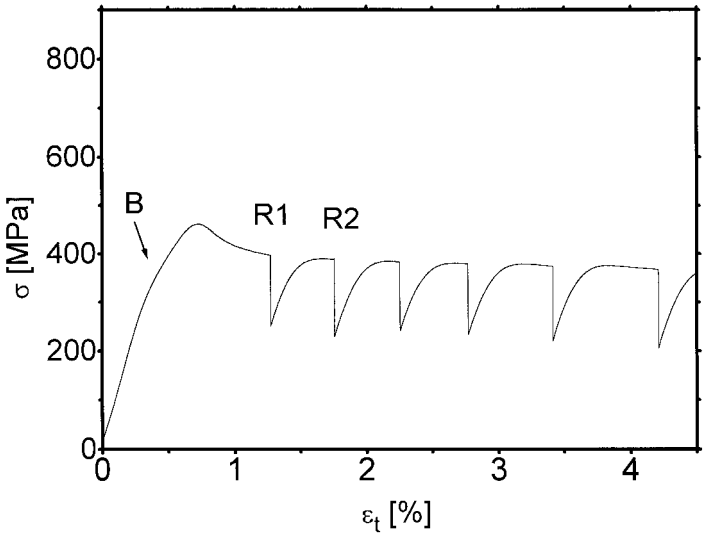

(*b*)

Figure 1. Stress–strain curves (i.e., σ versus total strain ε_t) of a specimen (*a*) with a fivefold compression axis deformed at 670°C and 656°C at a strain rate of $10^{-5}\,s^{-1}$ and (*b*) with a twofold compression axis deformed at 709°C at a strain rate of $10^{-5}\,s^{-1}$.

to record possible changes in the microstructure during the stress relaxation tests, 'repeated' relaxation tests (R2b in figure 1) were performed after an original relaxation (R2a) with the starting stress lower than the initial one so that only a small strain occurs and the steady state microstructure is not yet re-established. A few strain rate cycling tests were carried out to confirm the results of the stress relaxation tests. The temperature sensitivity $-(\Delta\sigma/\Delta T)_{\dot{\varepsilon}}$ of the flow stress was studied by temperature change tests (TC in figure 1 (*a*)). To change the temperature, it is necessary to partially unload the specimen (U in figure 1 (*a*)) to allow for thermal expansion or contraction. The time to reach thermal equilibrium after a change by 20 K was of the order of 30 min, i.e., the temperature changes are not 'instantaneous', in contrast to the strain rate changes. The procedure for determining the stress increment $\Delta\sigma$ owing to a temperature change is described in § 3.4.

§ 3. Results

3.1. *Shape of the stress–strain curves*

For first time, this study describes measurements of the deformation parameters of Al–Pd–Mn single quasicrystals below 680°C. Depending on the deformation conditions, a high-temperature range has to be distinguished from a low-temperature one. Figure 1 (*a,b*) shows the typical shapes of stress–strain curves of specimens with fivefold and twofold compression axes in the high-temperature range. The deformation behaviour is very similar for the two orientations. In figure 1 (*a*), stress relaxation curve R1 recorded before the yield point demonstrates that plastic deformation commences at loads far below the macroscopic yield stress. As figure 2 shows, a second relaxation performed immediately after the first one is shifted parallel to the stress axis to higher stresses, even at the relatively high temperature of 720°C. This shift can be interpreted as due to work-hardening. The work-hardening coefficient at

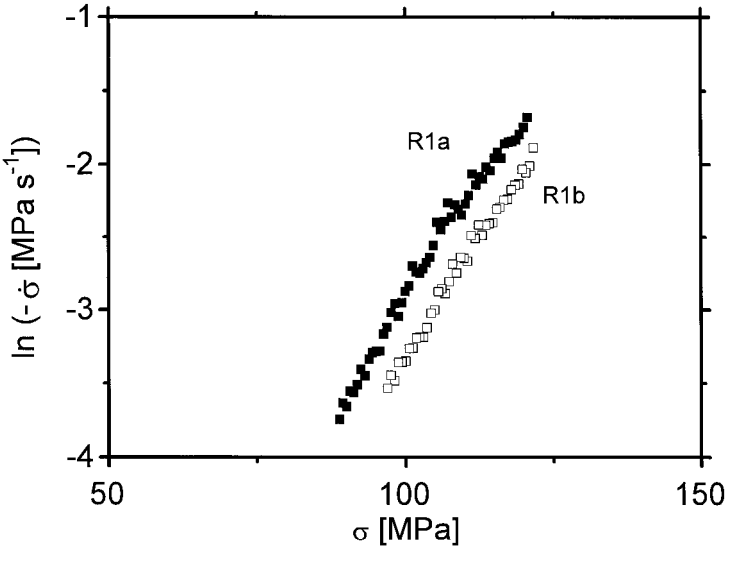

Figure 2. Original (R1a) and repeated (R1b) stress relaxation curves of a specimen with fivefold compression axis deformed at 720°C at a strain rate of $10^{-5}\,s^{-1}$, measured before the yield point at about one third of the yield stress.

constant relaxation rate $\Theta = \Delta a/\Delta\varepsilon$ can be obtained from the stress shift of the relaxation curves and the corresponding plastic strain, measured from the stress strain curves. In the 'preyield' region, it amounts to more than 10 GPa, with increasing values at decreasing temperatures. The range of rapid work-hardening is followed by an upper and a lower yield point. In many specimens of twofold orientation, a transition occurs across a narrow range of strain just before the upper yield point is reached from the quasi-elastic range to a distinct work-hardening range, leading to a 'bump' in the deformation curve, labelled B in figure 1 (*b*). The bump may occur also on re-loading after a stress relaxation test. A relaxation test performed within the bump always shows particular transient effects which will be described in § 3.3. The difference between the stresses at the upper and the lower yield point $\Delta\sigma|_{yp}$ increases with decreasing temperature, but the relative amplitude of the yield drops related to the stress at the lower yield point can be described by $\Delta\sigma|_{yp}/\sigma_{lyp} = -0.323 + 6.147 \times 10^{-4} T[^{\circ}\mathrm{C}]$, i.e., it decreases from about 0.18 at 820 °C down to 0.07 at 640 °C. The data show a large scatter, which is due to the fact that in many experiments stress relaxation tests were performed before the upper yield point, which influences the development of the yield drop effect. Yield point effects are observed also after stress relaxation tests or unloading. At the lower end of the high-temperature range, the yield point effects after deformation transients disappear. After the lower yield point, a plateau region follows up to about 5% plastic strain, where the work-hardening rate is slightly positive, zero or slightly negative, without a clear correlation to the deformation conditions. Deformation with strains larger than about 6% has not been investigated in this study. Deformation curves showing a yield drop followed by a range of almost zero work-hardening, which may correspond to a steady state of the dislocation structure, are characteristic of the high-temperature range described in this paper.

At the strain rates of $10^{-4}\,s^{-1}$ or $10^{-5}\,s^{-1}$ usually applied, the samples are brittle below certain temperatures, as pointed out in the next section. In order to achieve plastic deformation at lower temperatures, experiments have been performed at a nominal strain rate of $10^{-6}\,s^{-1}$ with stress relaxation experiments to prove the existence of plastic deformation at low temperatures. In these experiments, steady state conditions have not been attained. First results are described by Messerschmidt *et al.* (1999)

3.2. *Dependence of the flow stress on temperature, strain rate and orientation of the compression axis*

In figure 3, the temperature dependence of the flow stress at the plateau after the yield point is plotted for the high-temperature range of specimens with fivefold (full symbols) and twofold (open symbols) compression axes for strain rates of $10^{-4}\,s^{-1}$ (squares), and $10^{-5}\,s^{-1}$ (triangles). Specimens with a twofold compression axis break before they reach the upper yield point below about 700 °C at a strain rate of $10^{-5}\,s^{-1}$ and below about 715 °C at $10^{-4}\,s^{-1}$. The lowest temperature where deformation with a yield point effect followed by a steady state region was achieved was 635 °C at $10^{-5}\,s^{-1}$ for specimens with a fivefold compression axis. The different flow stresses for the two basic strain rates of $10^{-5}\,s^{-1}$ and $10^{-4}\,s^{-1}$ indicate a strong dependence of the flow stress on the strain rate. At the high-temperature end, specimens of both orientations show equal flow stresses. At lower temperatures, the flow stresses of the samples with twofold orientation are slightly lower than those of samples with fivefold orientation.

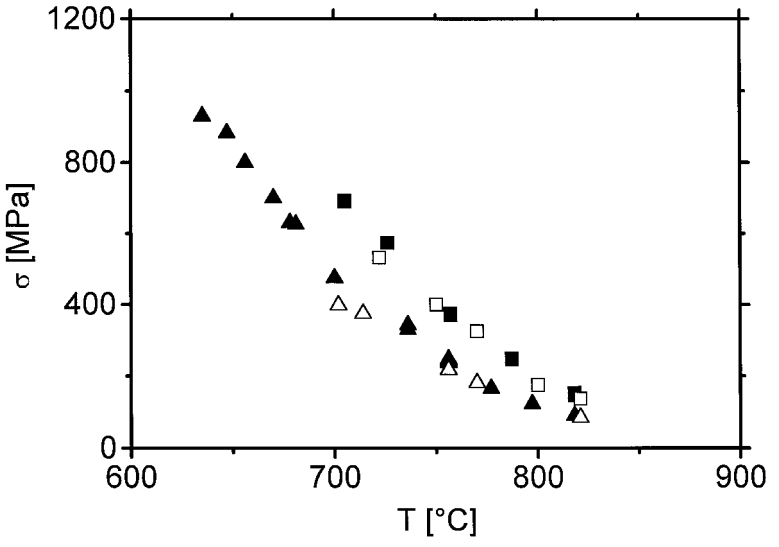

Figure 3. Temperature dependence of the flow stress σ in the plateau region of the stress–strain curve: filled symbols, fivefold orientation of the compression axis; open symbols, twofold orientation; triangles, strain rate of $10^{-5}\,s^{-1}$; squares, $10^{-4}\,s^{-1}$.

3.3. *Strain rate sensitivity of the flow stress*

The strain rate sensitivity was determined mainly by stress relaxation tests. To avoid the drastic changes in the microstructure during the yield point, most tests were performed within the range of steady state deformation. Curve R2a of figure 4 (*a*) shows a typical relaxation test at an intermediate temperature of 750°C starting from steady state deformation at the high strain rate of $10^{-4}\,s^{-1}$. The reciprocal slope of these curves equals the experimental strain rate sensitivity r_{ex} as described in § 2. The initial slope corresponds to the strain rate before the relaxation test. The curve shows the commonly observed positive curvature, i.e., decreasing strain rate sensitivity with decreasing stress or strain rate. For relaxation times of a few minutes, about half of the flow stress relaxes at a starting strain rate of $10^{-4}\,s^{-1}$. Curve R2a in figure 4 (*b*), taken at 820°C, demonstrates that the shape of the relaxation curves remains the same at higher temperatures also. At lower temperatures, the stress relaxation curves become almost straight, as shown by curves R1a and R2a in figure 4 (*c*), measured at 700°C and 678°C, respectively. The strain rate sensitivity in the plateau region of the deformation curves is almost independent of the strain within the range of the present experiments, i.e., up to about 6% plastic strain.

To check the consistency of the strain rate sensitivity data taken under the same stress but at different temperatures and strain rates, r_{ex} values were determined not only at the beginning of the relaxation curves, but also along a long relaxation curve, as already pointed out in § 2. These data will be presented and discussed in § 5 of Part II (Messerschmidt *et al.* 2000).

In order to assess changes in the microstructure during the relaxation tests, original relaxation tests labelled RXa were followed by further relaxations after reloading the specimens to a load slightly below that of the original relaxations, as described in § 2 and depicted in figure 1 (*a*). These *repeated* relaxations are labelled RXb. As shown in figure 4 (*b*), the repeated relaxation curves fall below the original

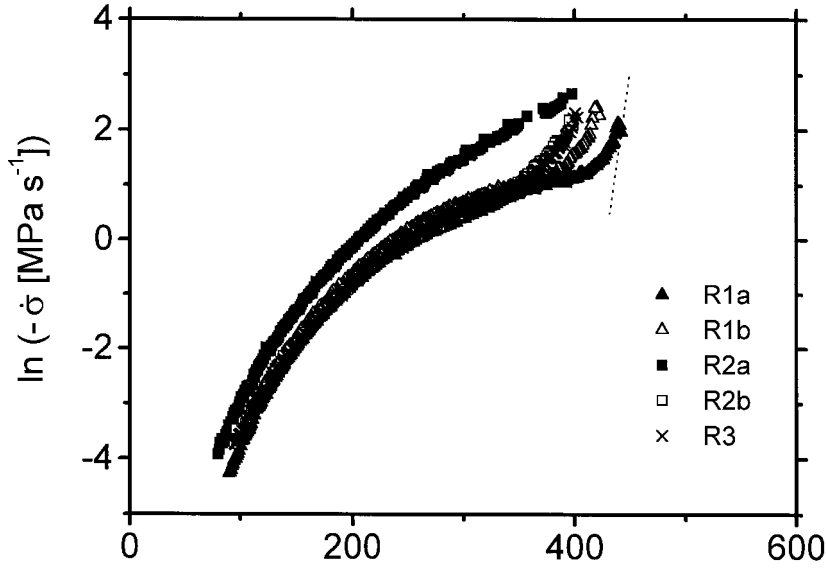

(*a*)

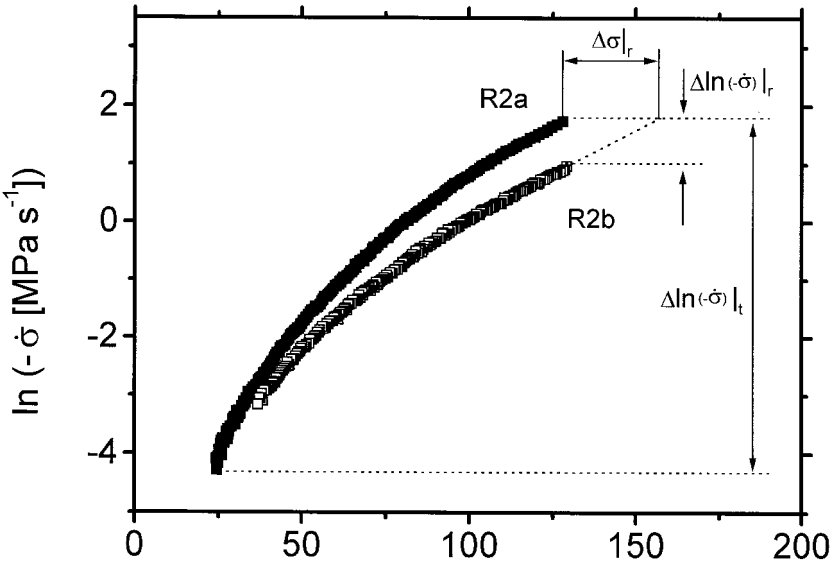

(*b*)

Figure 4. Stress relaxation curves under different experimental conditions. (*a*) Specimen of twofold orientation of the compression axis deformed at 750°C at a strain rate of $10^{-4}\,s^{-1}$. R1a and R1b are relaxation and repeated relaxation curves taken just before the upper yield point. R2a and R2b are relaxation and repeated relaxation curves taken in the plateau region at about 2% plastic strain. R3 is a relaxation curve taken in the plateau region at about 3.6% plastic strain after unloading for 20 min and reloading as for a repeated relaxation. (*b*) Specimen of fivefold orientation during deformation at 820°C at a strain rate of $10^{-4}\,s^{-1}$. $\Delta\sigma|_r$, $\Delta \ln(-\dot{\sigma})|_r$ and $\Delta \ln(-\dot{\sigma})|_t$ are described in the text. (*c*) Specimen of fivefold orientation during deformation at 700°C (R1a and R1b) and after a temperature change down to 678°C (R2a and R2b) at a strain rate of $10^{-5}\,s^{-1}$. Here r_{ex1} and r_{ex2} are the inverse slopes of curves R1a and R2a.

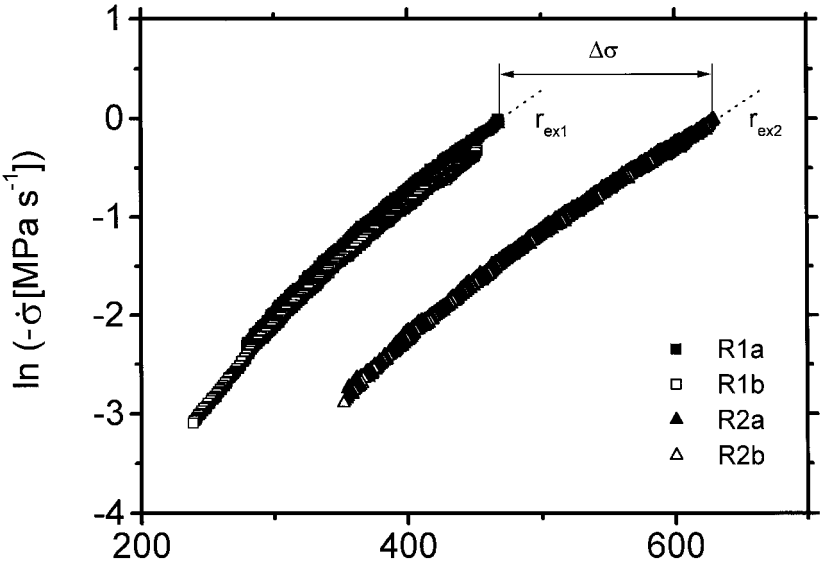

(*c*)

Figure 4. (*Continued*)

curves, i.e., the strain rates are lower for equal stresses. At the lower end, i.e., after long relaxation times leading to low strain rates, the original and repeated relaxation curves coincide. The difference between the original and repeated relaxation curves decreases with decreasing temperature, as becomes obvious from figure 4(*b,c*). Further repeating the stress relaxation tests without reaching the steady state stress does not cause additional changes, i.e., the first repeated relaxation and the following ones follow the same curve. Thus, original relaxation curves coincide with each other and repeated relaxation curves after long relaxations, too, but original relaxations do not coincide with repeated ones owing to the yield drop effect between them.

At the lower part of the high-temperature region, the original and repeated relaxation curves measured before the yield point do not meet at low relaxation rates. Instead, they are shifted with respect to each other parallel to the stress axis, as demonstrated in figure 2. This was explained in §3.1 by work-hardening during the relaxations.

A parameter C_r is defined as a quantitative measure of the differences between the original and the repeated relaxation curves, which correspond to differences in the starting microstructures. As these differences increase with increasing relaxation times, this parameter relates the difference in the relaxation rates between the original and repeated relaxations $\Delta \ln(-\dot{\sigma})|_r$ at the beginning of the relaxations to the total change $\Delta \ln(-\dot{\sigma})|_t$ of the relaxation rate during the original relaxation, as indicated in figure 4(*b*):

$$C_r = \Delta \ln(-\dot{\sigma})|_r / \Delta \ln(-\dot{\sigma})|_t. \quad (2)$$

In figure 5, the experimental values of C_r are plotted as a function of the deformation temperature. Within the framework of the relatively few data points, C_r seems to be independent of the strain rate and the specimen orientation. A linear regression

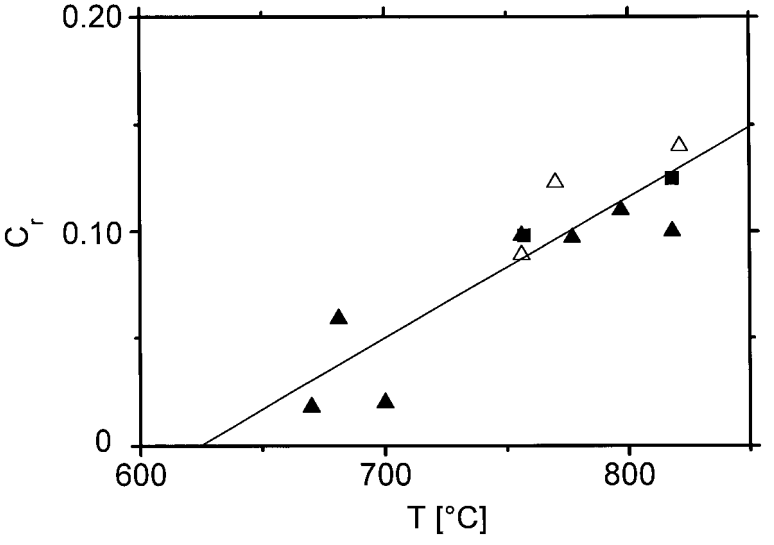

Figure 5. Dependence of the recovery parameter C_r on the temperature (symbols as in figure 3).

analysis of all data points yields

$$C_r = -0.42 + 6.6 \times 10^{-4} T\,[^{\circ}\mathrm{C}], \tag{3}$$

which crosses the abscissa at about 625°C. Thus, structural changes during stress relaxation tests are negligible only at the lowest temperature within the high-temperature deformation range.

The microstructural changes during the relaxations cause a yield drop effect with a stress difference $\Delta\sigma|_{ypr}$ if the specimen is reloaded until a new steady state deformation is reached, as demonstrated in figure 6 (*a*). Figure 6 (*b*) compares this difference with the extrapolated stress difference $\Delta\sigma|_r$ between the original and the repeated relaxation curves defined in figure 4 (*b*), demonstrating that the two differences are almost equal. The straight line in figure 6 (*b*) is the result of a linear regression forced through the origin. It has a slope of 0.9, i.e., close to unity.

Figure 7 (*a*) is a compilation of the experimental strain rate sensitivity data. The values correspond to the starting points of (original) relaxation tests performed in the plateau regions of the stress–strain curves. Data points with the same symbol at the same temperature originate from a single specimen. The strain rate sensitivity increases dramatically with decreasing temperature and seems to reach a constant value at the lowest temperature of macroscopic deformation. The strain rate sensitivity tends to increase with higher strain rates. As for the flow stress, the specimen orientation is of little influence. In order to check the results of the stress relaxation tests, a few strain rate cycling tests were performed from a strain rate of $10^{-5}\,s^{-1}$ to one of $10^{-4}\,s^{-1}$ (asterisks in figure 7 (*a*)). They have to be attributed to an average strain rate of $\sqrt{10^{-5} \times 10^{-4}}\,s^{-1} \cong 3.2 \times 10^{-5} s^{-1}$ and fit quite well to the results of relaxation tests if the stress increment is measured between the steady state stress at $10^{-5}\,s^{-1}$ and the upper yield point at $10^{-4}\,s^{-1}$.

Particular transient effects occur if stress relaxation tests are started at a state of non-constant internal structure as, e.g., before the upper yield point, where the

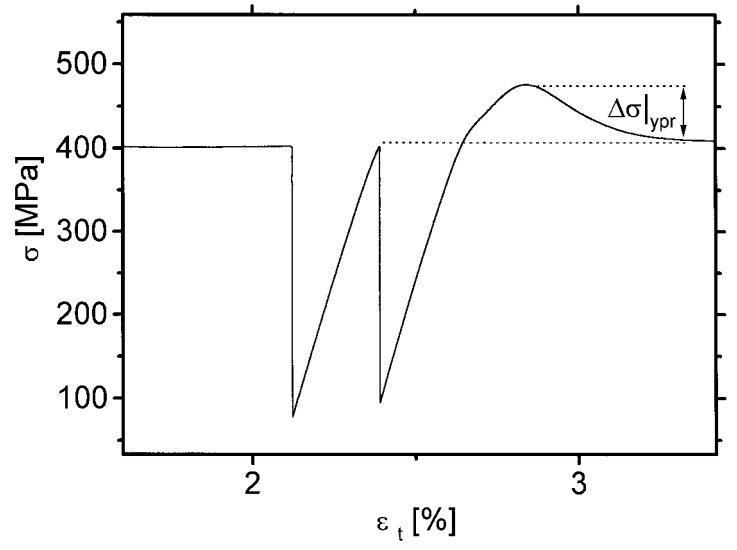

(*a*)

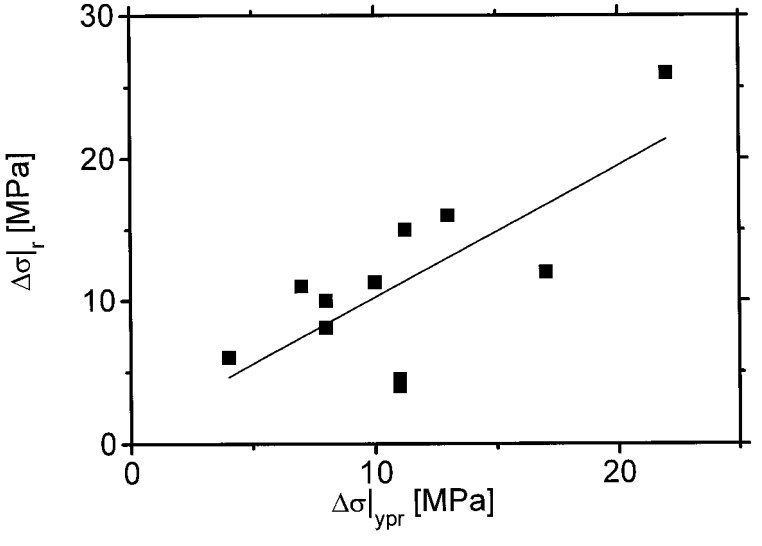

(*b*)

Figure 6. Transient effects during reloading after a stress relaxation test: (*a*) yield drop in the stress-strain curve; and (*b*) dependence of the stress difference of the yield drop $\Delta\sigma|_{yp}$ on the stress difference $\Delta\sigma|_r$ between the original and the repeated relaxation curves.

specimen undergoes strong work-hardening. The relaxation curve may then exhibit an additional part of low strain rate sensitivity at the beginning of the relaxation test as curve R1a in figure 4(*a*). This initial part leads to an 'inverse' curvature of the relaxation curve at the beginning of the relaxation test. Relaxation curves with an inverse curvature at the beginning may appear also during repeated relaxations. This is demonstrated in figure 4(*a*) by the curves R1b for a 'preyield' curve, and R2b for a

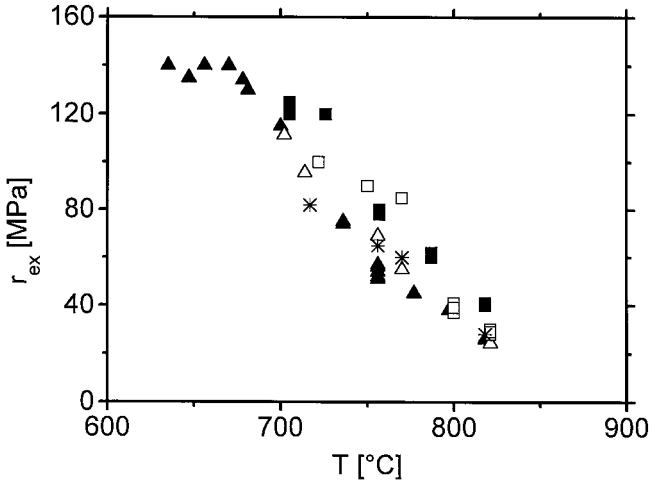

(*a*)

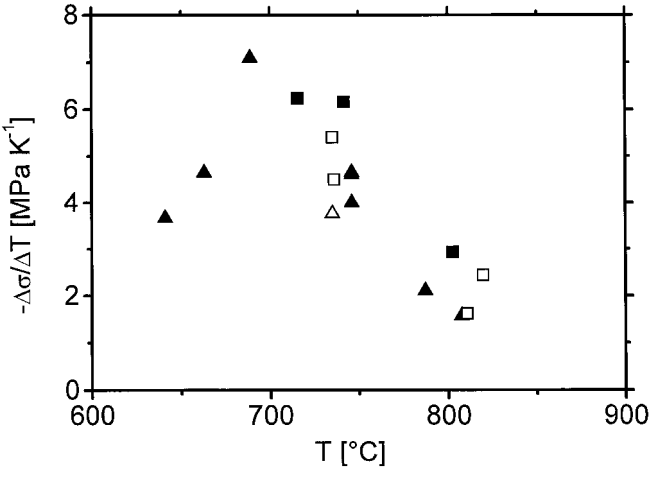

(*b*)

Figure 7. Dependence of the strain rate and stress sensitivities of the flow stress on temperature (symbols as in figure 3). (*a*) Strain rate sensitivity r_{ex} measured at the beginning of original relaxation tests in the plateau region of the stress–strain curve: asterisks are strain rate cycling tests on specimens with fivefold compression axis from $10^{-5}\,s^{-1}$ to $10^{-4}\,s^{-1}$, corresponding to an average strain rate of $3.2 \times 10^{-5}\,s^{-1}$. (*b*) Temperature sensitivity of the flow stress.

repeated relaxation in the plateau region. Sections with inverse curvature appear whenever the specimen is loaded close to the starting load of the original relaxation. They are particularly pronounced if the stress–strain curves show a 'bump' like B in figure 1 (*b*). They appear also after unloading, as shown by curve R3 in figure 4(*a*). The strain rate sensitivities corresponding to the parts with inverse curvature of the relaxation curves either from tests before the upper yield point or from repeated relaxations are of an order of magnitude of only 10–30 MPa.

3.4. *Temperature sensitivity of the flow stress*

The temperature sensitivity of the flow stress $-(\Delta\sigma/\Delta T)_{\dot{\varepsilon}}$ was determined from temperature change experiments. As described in § 2, the temperature changes are never 'instantaneous' changes. Therefore, in this study the stress increments $\Delta\sigma$ were determined between steady state stresses taken at the beginning of original stress relaxation tests before and after the temperature change, as described in figure 4 (*c*). The stress increments are assigned to the average temperature. In figure 7 (*b*), the temperature sensitivity of the flow stress $-(\Delta\sigma/\Delta T)_{\dot{\varepsilon}}$ is plotted as a function of the temperature. It does not seem to depend on the orientation of the compression axis. Above 700°C, it decreases rapidly with increasing temperature. Below 700°C, data are available only for the fivefold orientation. There, the temperature sensitivity decreases with decreasing temperature. The temperature sensitivity data from temperature change tests agree well with the slope of the plot of the steady state flow stress versus temperature in figure 3. Here, even the decrease at the lowest temperatures is indicated.

§ 4. Conclusion

At a strain rate of $10^{-5}\,s^{-1}$ above about 640°C, Al–Pd–Mn single quasicrystals show a region of almost steady state deformation after an upper and a lower yield point. Both the flow stress in the steady state region and its strain rate sensitivity decrease strongly with increasing temperature. The data are almost equal for specimens of twofold and fivefold compression axes.

Repeated relaxation curves following an original relaxation after reloading to a stress slightly lower than the plateau stress level do not coincide with the original relaxations. This points to changes in the dislocation structure occurring during the relaxation tests. The effect decreases with decreasing temperature and disappears at about 625°C.

Transient effects in the form of an inverse curvature at the beginning of the relaxation tests are observed also if relaxation curves are started from a non-steady-state deformation, e.g., during loading before the yield point, after long relaxation tests or after unloading.

References

Bresson, L., and Gratias, D., 1993, *J. non-crystalline Solids,* **153–154**, 468.

Brunner, D., Plachke, D., and Carstanjen, H. D., 1997, *Mater. Sci. Eng.* A, **234–236**, 310.

Feuerbacher, M., Baufeld, B., Rosenfeld, R., Bartsch, M., Hanke, G., Beyss, M., Wollgarten, M., Messerschmidt, U., and Urban, K., 1995, *Phil. Mag. Lett.,* **71**, 91.

Feuerbacher, M., Metzmacher, C., Wollgarten, M., Urban, K., Baufeld, B., Bartsch, M., and Messerschmidt, U., 1997, *Mater. Sci. Eng.* A, **233**, 103.

Messerschmidt, U., Bartsch, M., Geyer, B., Feuerbacher, M., and Urban, K., 2000, *Phil. Mag.* A, **80**, 1165.

Messerschmidt, U., Geyer, B., Bartsch, M., Feuerbacher, M., and Urban, K., 1999, *Quasicrystals,* MRS Proceedings Vol. 553 (Pittsburgh, PA: Materials Research Society), p. 319.

Schall, P., Feuerbacher, M., Messerschmidt, U., and Urban, K., 1999, *Phil. Mag. Lett.,* **79**, 785.

Shibuya, T., Hashimoto, T., and Takeuchi, S., 1990, *Jap. J. appl. Phys.,* **29**, 349.

Shield, J. E., Kramer, M. J., and McCallum, R. W., 1994, *J. Mater. Res.,* **9**, 343.

Takeuchi, S., and Hashimoto, X., 1993, *Japan J. appl. Phys.,* **30**, 561.

Tsai, A. P., Inoue, A., and Masumoto, T., 1989, *Mater. Trans Jap. Inst. Metals,* **30**, 666.

WOLLGARTEN, M., BARTSCH, M., MESSERSCHMIDT, U., FEUERBACHER, M., ROSENFELD, R., BEYSS, M., and URBAN, K., 1995, *Phil. Mag. Lett.,* **71**, 99.
WOLLGARTEN, M., BEYSS, M., URBAN, K., LIEBERTZ, H., and KÖSTER, U., 1993, *Phys. Rev. Lett.,* **71**, 549.
YOKOYAMA, Y., MIURA, T., TSAI, A. P., INOUE, A., and MASUMOTO, T., 1992, *Mater. Trans. Jap. Inst. Metals,* **33**, 97.